Materials Science Forum Vol. 762 (2013) pp 295-300
Online available since 2013/Jul/01 at www.scientific.net

doi:10.4028/www.scientific.net/MSF.762.295

Modelling of Grain Refinement Induced by SMAT Process, Using a Complete Numerical Chaining Methodology

S. Benafia[1,a], D. Retraint[1,b], B. Panicaud[1,c], L. Le Joncour[1,d], E. Rouhaud[1,e] and M. Micoulaut[2,f]

[1] ICD – LASMIS, Université de Technologie de Troyes (UTT),

12 rues Marie Curie,10010 Troyes, France

[2] LPTMC, Université Pierre et Marie Curie (UPMC), 4 place Jussieu, 75252 Paris, France

[a]souhail.ben_afia@utt.fr, [b]delphine.retraint@utt.fr, [c]benoit.panicaud@utt.fr, [d]lea.le_joncour@utt.fr, [e]emmanuelle.rouhaud@utt.fr, [f]mmi@lptl.jussieu.fr

Keywords: Surface Mechanical Attrition Treatment / Finite Element simulation / Shot velocity / Grain refinement

Abstract. Surface Mechanical Attrition Treatment (SMAT) is a recent process that enables to nanocrystallise the surface of metallic alloys. It can thus enhance mechanical properties of the treated material by inducing a grain refinement down to the nanometre scale, in the top surface layer. This nanocrystallisation process leads to different effects that were successively studied on several metallic materials. In the present work, investigations are carried out on the modelling of SMAT. A simulation of the shot dynamics is performed using different process parameters, with the aim to obtain the impact velocity field on the treated surface. This field is then used as an input for a finite element model to predict the induced grain refinement. The evolution of the micro and nanostructures are then calculated using a micromechanical approach, which takes into account the dislocations and their interactions. Coupled with a finite element analysis, this approach enables to deduce the influence of the process on the macroscopic material properties, whatever the geometry of the sample.

Introduction

The Surface Mechanical Attrition Treatment (SMAT) is a mechanical process consisting of projecting shots, i.e. small steel balls on a metallic sample. During this process, shots, contained in a peening chamber, are propelled by a sonotrode and impact the surface of the workpiece causing severe plastic deformation. Several impacts induce multiple effects on the treated surface such as the generation of compressive residual stresses, refined grained layers and a hardening of the near surface layer [1]. It can thus improve the mechanical behaviour, such as the fatigue properties [2], besides also the corrosion resistance of the metal [3]. The residual stress field and the characteristics of the nanostructured layer depend strongly on some parameters of the process, such as shot impact velocities, impact angles and surface coverage. These parameters themselves depend on the chosen setup parameters, such as the amplitude of the sonotrode vibration, the shot diameter, the geometry of the peening chamber, etc. It should also be noted that SMAT results depend strongly on the type of material sample, which can be explained by the corelation between refinement mechanisms and the physical and mechanical properties of materials. Therefore, the mechanisms responsible for the grain refinement under SMAT treatment are not yet fully understood.

The aim of this study is to investigate the grain refinement with respect to the shot peeing process parameters. Actually, experimental methods can be carried out but are unfortunately time-consuming whereas the nature of the shot trajectories cannot be fully characterized. To circumvent this problem, extensive analytical 3D models for shot dynamics within the SMAT process is performed and enables to predict the impact velocity field, which will be used as input in further simulations. Besides, a micromechanical approach coupled with a finite element analysis is developed giving the evolution of the micro and nanostructures in the treated sample, which takes

into account dislocations and their interactions. In the present article, the first step of the numerical methodology will be presented, whereas only a qualitative description of the methodology will be provided for the second and third steps.

Complete numerical chaining methodology

The complete numerical chaining method is described in Figure 1 and applied to a cylinder-shaped sample. Following this approach, it is possible to obtain a prediction of the grain refinement on the peened part as a function of the process parameters and material properties. Velocity and impact angles obtained by the shot dynamic model are used in the second step as input for a finite element simulation. From this analysis, the displacement resulting from the impacts simulation will be used in another finite element modelling coupled to a micromechanical approach taking into account different dislocation densities in order to predict the grain refinement.

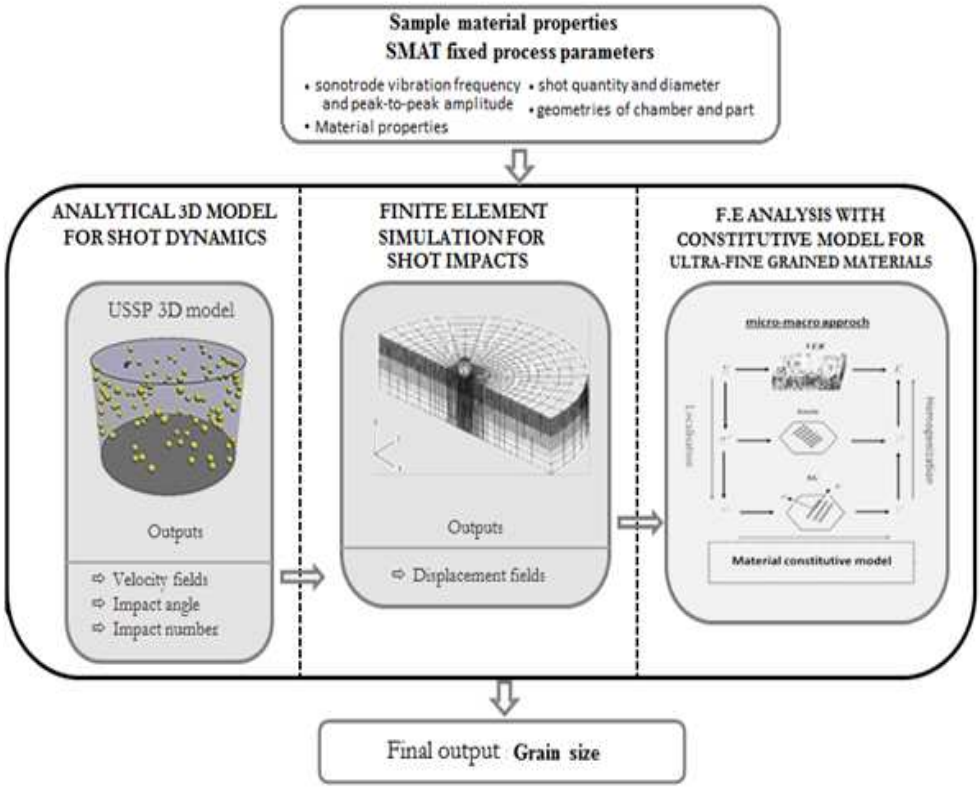

Fig. 1 - General numerical chaining methodology

Analytical 3D model for shot dynamics

The aim of the first stage of this approach is to extract the impact velocity field and the impact angles distribution after simulating the shot dynamics, with the chosen experimental setup parameters of the process. The model of the shot dynamics is based on a model that was originally created for granular gases [5], whereas the inputs of the model correspond to the experimental parameters:

- The sonotrode vibration frequency and the peak-to-peak amplitude, the excitation profile being triangular;
- The material properties of the shot, of the sonotrode, of the part and of the chamber;
- Shot quantity and diameter;
- The chamber and the part geometries.

The model used in this step (Figure 2-a) simulates the dynamics of hard spheres placed in a cylindrical chamber (or in a plane-parallel box as shown in Figure 2-b) and propelled by a vibrating membrane against a flat surface. As mentioned earlier, these spheres represent the shot.

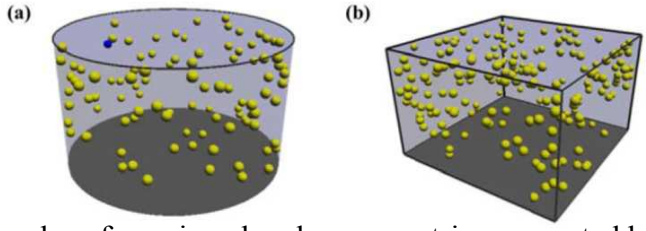

Fig. 2 - Examples of peening chamber geometries supported by the model: a) cylinder b) plane-parallel box

Based on an event-driven algorithm [5], the model provides the trajectory of each sphere and saves impacts result data such as the type and the instant of the impact, its 3D coordinates, as well as its impact and rebound velocities. The model detects "shot-shot" and "shot-wall" impacts and takes into account energy dissipation during impact through normal and tangential restitution coefficients. By simulating thousands of impacts onto the treated part, we have been able to calculate impact velocity and impact angle distribution from statistical averages as discussed below and represented in these figures.

Chamber diameter D = 70 mm	Height of the chamber H = 45 mm	Shot diameter Ø = 3 mm	Shot quantity Q = 20 g	Vibration frequency of the sonotrode Fr = 20 kHz

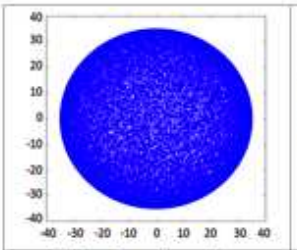

Fig. 3 - Spatial impact distribution

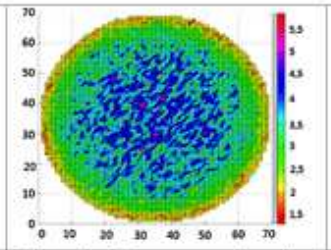

Fig. 4 - Impact velocity distribution (m/s)

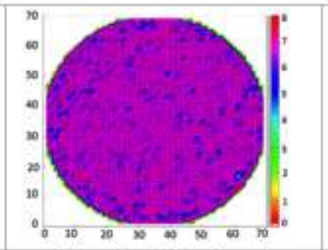

Fig. 5 - Maximal velocity distribution (m/s)

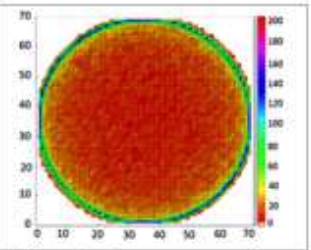

Fig. 6 - Impact number distribution

Here, the surface of the peened sample is divided into small elements using a grid of base (1mm×1mm). In each element of that grid, the average impact velocity of all impacts is calculated, as well as the impact number and the maximal velocity (see also Fig. 5). The impact velocity corresponds to the norm of all components of shot velocity, and it is found that its distribution is heterogeneous (Figure 4). This contrasts with the distribution of the maximal velocity that appears to be much more homogeneous (Figure 5). As shown in Figure 4, it can also be noted that the impact velocity is higher in the centre of the sample (5.5 m/s) than in the edges of the chamber (2 m/s). If we consider now the impact numbers, we can note that as one gets closer to the borders, the number of impacts increases (Figure 6). This behaviour can be explained by the fact that the impacts at the border and the side walls decrease the velocity of the shot.

The impact velocity distribution on the treated sample, for different values of sonotrode vibration amplitude, is presented in Figure 7. This distribution corresponds to the percentage of impact for different velocities defined between zero and the maximum velocity (e.g. 2m/s for 6µm of sonotrode amplitude). This figure shows the existence of two velocity peaks. We can also see that an increase of the sonotrode amplitude provides a decrease in the peak percentage, but an increase of the corresponding velocity. The overall shape of the present distribution is driven by the triangular excitation profile. For the case of infinite dilution, it would select only two possible

impact velocities arising from the downward and upward motion of the sonotrode, and lead to a bimodal distribution for the impact percentage. However, given the shot density and the disorder induced by various collisions, the obtained impact profile is only a weak reminiscence of such a bimodal distribution.

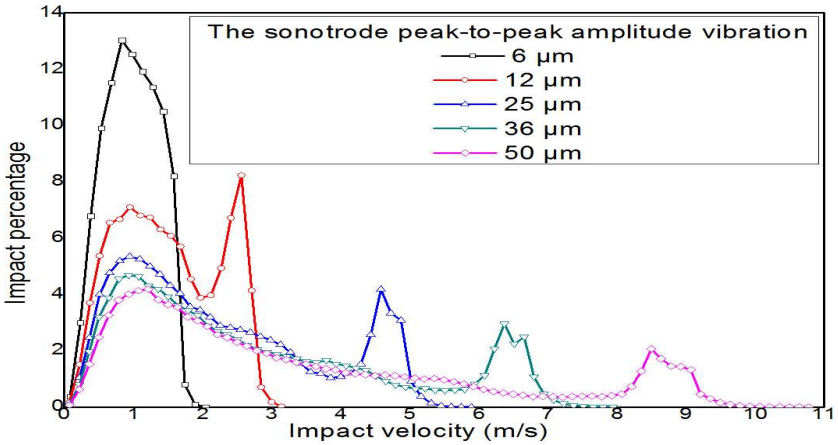

Fig. 7 - Influence of the sonotrode amplitude vibration on the impact percentage vs. impact velocity

Finite Element simulation for shot impacts

The results obtained by the shot dynamic model are used in this second step as an input for a finite element analysis. First, the finite element model is developed to investigate single and multiple impacts effects on a target using the commercial finite element code ABAQUS Explicit. The simulation has been carried out by using a three dimensional finite element applied to an elastoplastic model. The material sample is a 316L steel.

One shot with a diameter of 3 mm, similar to the shot used in the analytical 3D model for shot dynamics, is modelled as a rigid sphere and defined by a reference point corresponding to its centre. Impact velocity and impact angle were defined as boundary conditions, in accordance with the angle and velocity distributions extracted from the shot dynamic model. General Coulomb contact was used as the criteria of contact with an isotropic friction coefficient equal to 0.3. Taking into account symmetries, only one half of the circular plate was analysed. The part was restrained against all displacements and rotations on the bottom. Convergence tests were conducted using different meshes and element types to ensure the numerical results.

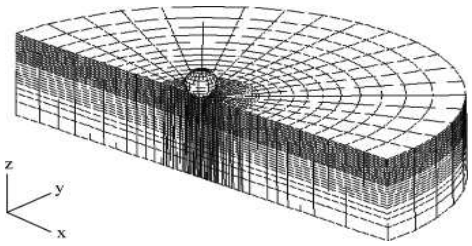

Fig. 8 - Three-dimensional FE model for a single shot impacting on a target.

The aim of this step is to recover the resulting displacement fields after the shot impacts. These displacement fields are used as boundary conditions in another finite element simulation based on a micromechanical approach. For the latter, the dislocation density-based material model subroutines defined further are incorporated in a finite element modelling to calculate the dislocation fields in the work piece over a single or multiple impacts.

Constitutive model for ultra-fine grained materials

The third step consists of using the above results in order to predict the grain refinement. In this topic, various studies have been already done. For example, the model of grain refinement presented by Estrin et al. [7] suggests evaluating the dislocation density evolution rates from a set of differential equations. Their dislocation density-based material model was applied in the ECAP (Equal-Channel Angular Pressing) processes onto various materials such as aluminium [6], copper [7] and interstitial-free steel [8]. Based on the same evolution equations, other constitutive models have been adapted to model subsurface grain refinement for different deformation processes with high strain rates or high temperature gradients such as Taylor impact test of copper [9], laser-induced shock compression [10] and orthogonal cutting of aluminium [11]. In this section, we shall restrict ourselves to a general presentation of the main equations defining the model that can be adapted.

In such models, dislocation structures are supposed to be formed during deformation. Therefore, the material can be conceived as a two-phase composite consisting of cell walls of high dislocation density and cell interiors which are relatively low in dislocation density. Two types of dislocation densities are then proposed in the present model: the cell interior dislocation density ρ_c and the cell wall dislocation density ρ_w. The average dislocation densities of the two phases introduced above determine the total dislocation density ρ_t. The average cell size d is assumed to scale with the inverse of the square root of ρ_t:

$$d = \frac{K}{\sqrt{\rho_t}} \tag{1}$$

$$\rho_t = f\ \rho_w + \left(1 - f\ \right)\rho_c \tag{2}$$

where K is a constant depending on the used material, f is the volume fraction of the walls. f_0 is the initial value of f, f_∞ is its saturation value and γ^r describes the variation of f with the resolved shear strain. The quantity $\tilde{\gamma}$ describes the rate of decrease of f:

$$f = f_\infty + (f_0 - f_\infty)\exp(\frac{-\gamma^r}{\tilde{\gamma}}) \tag{3}$$

This particular form of the volume fraction, with f_0 taken to be larger than f_∞, implies that the walls become sharper as the strain increases in the material. This sharpening outstrips the concurrent increase in cell boundary area with cell size reduction.

The evolutions of the dislocation densities ρ_c and ρ_w are governed by the following equations:

$$\dot{\rho}_c = \frac{\alpha^* \dot{\gamma}^r \sqrt{\rho_w}}{\sqrt{3}b} - \frac{6\beta^* \dot{\gamma}^r}{bd\left(1-f\right)^{1/3}} - k_0 \left(\frac{\dot{\gamma}^r}{\dot{\gamma}_0}\right)^{-1/n^*} \dot{\gamma}^r \rho_c \tag{4}$$

$$\dot{\rho}_w = \frac{\sqrt{3}\beta^* \dot{\gamma}^r \left(1-f\right)\sqrt{\rho_w}}{fb} + \frac{6\beta^* \dot{\gamma}^r \left(1-f\right)^{2/3}}{d\ b\ f} - k_0 \left(\frac{\dot{\gamma}^r}{\dot{\gamma}_0}\right)^{-1/n^*} \dot{\gamma}^r \rho_w \tag{5}$$

α^*, β^* and k_0 are parameters of the material controlling the dislocation evolution rate, n is a temperature sensitivity parameter, d is the dislocation cell size, b is the magnitude of the Burgers vector of the considered material, $\dot{\gamma}^r$ is the resolved shear strain which can be calculated by the von Mises strain rate $\dot{\gamma}^r = \mathrm{M}\,\dot{\varepsilon}$, where M is the Schmidt tensor.

The set of equations presented in this section define the constitutive material behaviour based on the physical mechanisms operating at the scale of dislocations. These equations can then be introduced into a general micromechanical model. The main advantage of the approach using a scale transition model is its ability to predict the evolution of the microstructure (represented by the dislocation density and cell/particle size).

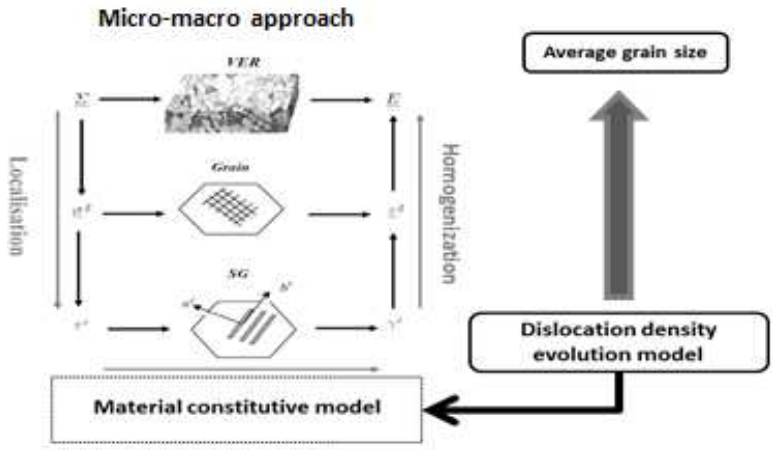

Fig. 9 - Micromechanical approach using a dislocation evolution model

Conclusions

In this paper, we have presented a general methodology that allows a linking of SMAT process parameters and their corresponding induced grain refinement. In the first step, by simulating multiple impacts, statistical studies for impact number and velocity have been performed. It could be noted that the impact velocity is higher in the centre of the sample and the number of impacts increases near the borders. The study of heterogeneity is thus of primary importance for such a process. The investigation is carried out with different sonotrode vibration amplitudes. It thus shows the same conclusions with two velocity peaks. A dislocation density-based predictive model can also be adapted with a micromechanical approach to simulate the high-strain rate plastic deformation and microstructural evolution under the repetitive impacts of the SMAT process. More studies will be conducted to test the limits and performance of this numerical chaining methodology.

References

[1] T. Roland, D. Retraint, J. Lu, K. Lu, Mater. Sci. Forum 490-491 (2005) 625-630.
[2] J. Uusitalo, L.P. Karjalainen, D. Retraint, M. Palosaari, Mater. Sci. Forum 604–605 (2009) 239-248.
[3] B. Panicaud, Retraint, J.-L. Grosseau-Poussard, L. Li, M. Guérain, P. Goudeau, N. Tamura, M. Kunz, Cor. Sci. 60 (2012) 224–230.
[4] Y. Estrin, H. S. Kim, Mater. Sci. 42 (2007) 1512-1516.
[5] M. Micoulaut, S. Mechkov, D. Retraint, P. Viot, M. François, Granul. Matter. 9 (2007) 25-33.
[6] S.C. Baik, Y. Estrin, H.S. Kim, R.J. Hellmig, Mat. Sci. Eng. A 351 (2003) 86-97.
[7] S.C. Baik, R.J. Hellmig, Y. Estrin, H.S. Kim, Z Metallkd. 94 (2003) 754-760.
[8] S.C. Baik, Y. Estrin, H.S. Kim, H.T. Jeong, R.J. Hellmig, Mat. Sci. Forum 408-412 (2002) 697-702.
[9] V. Lemiale, Y. Estrin, H.S. Kim, R. O'Donnell, Comp. Mat. Sci. 48 (2010) 124-132.
[10] H. Ding, Y.C. Shin, Comp. Mat. Sci. 53 (2012) 79-88.
[11] H. Ding, N. Shen, Y.C. Shin, Comp. Mat. Sci. 50 (2011) 3016-3025.

Physical and Numerical Simulation of Materials Processing VII
10.4028/www.scientific.net/MSF.762

Modelling of Grain Refinement Induced by SMAT Process, Using a Complete Numerical Chaining Methodology

10.4028/www.scientific.net/MSF.762.295